Temperature dependence of the magnetic susceptibility for triangular-lattice antiferromagnets with spatially anisotropic exchange constants

Weihong Zheng,[1] Rajiv R. P. Singh,[2] Ross H. McKenzie,[3] and Radu Coldea[4]
[1]*School of Physics, University of New South Wales, Sydney NSW 2052, Australia*
[2]*Department of Physics, University of California, Davis, California 95616, USA*
[3]*Department of Physics, University of Queensland, Brisbane, Australia*
[4]*Department of Physics, Oxford University, Oxford OX1 3PU, United Kingdom*
(Received 14 October 2004; published 27 April 2005)

We present the temperature dependence of the uniform susceptibility of spin-half quantum antiferromagnets on spatially anisotropic triangular lattices, using high-temperature series expansions. We consider a model with two exchange constants J_1 and J_2 on a lattice that interpolates between the limits of a square lattice ($J_1=0$), a triangular lattice ($J_2=J_1$), and decoupled linear chains ($J_2=0$). In all cases, the susceptibility, which has a Curie-Weiss behavior at high temperatures, rolls over and begins to decrease below a peak temperature T_p. Scaling the exchange constants to get the same peak temperature shows that the susceptibilities for the square lattice and linear chain limits have similar magnitudes near the peak. Maximum deviation arises near the triangular-lattice limit, where frustration leads to much smaller susceptibility and with a flatter temperature dependence. We compare our results to the inorganic materials Cs_2CuCl_4 and Cs_2CuBr_4 and to a number of organic molecular crystals. We find that the former (Cs_2CuCl_4 and Cs_2CuBr_4) are weakly frustrated and their exchange parameters determined through the temperature dependence of the susceptibility are in agreement with neutron-scattering measurements. In contrast, the organic materials considered are strongly frustrated with exchange parameters near the isotropic triangular-lattice limit.

DOI: 10.1103/PhysRevB.71.134422 PACS number(s): 75.10.Jm, 75.50.Ee

I. INTRODUCTION

Understanding the interplay of quantum and thermal fluctuations and geometrical frustration in low-dimensional quantum antiferromagnets is a considerable theoretical challenge.[1–6] Research in frustrated quantum antiferromagnets was greatly stimulated by Anderson's "resonating valence bond" (RVB) paper[7] in which he suggested that the parent insulators of the cuprate superconductors might have spin liquid ground states and excitations with fractional quantum numbers, motivated by his earlier suggestion of such a ground state for the Heisenberg antiferromagnet on the triangular lattice.[8] The Ising model on a triangular lattice illustrates the rich physics that can arise due to frustration: it is known to have a macroscopic number of degenerate ground states.[9] The antiferromagnetic Heisenberg model with spatially anisotropic exchange interactions on the triangular lattice is of interest both theoretically and experimentally. It describes the spin excitations in Cs_2CuCl_4 (Ref. 10) and Cs_2CuBr_4 (Ref. 11) and the Mott insulating phase of several classes of superconducting organic molecular crystals.[12] Other materials for which this model is relevant include $NaTiO_2$,[13] $CuCl_2$ graphite intercalation compounds,[14] and the anhydrous alum, $KTi(SO_4)_2$.[15] Theoretically, this Heisenberg model is a candidate for a system with spin liquid ground states and possibly excitations with fractional quantum numbers.[8,16,17] For the triangular-lattice model with spatially isotropic interactions, the preponderence of numerical evidence[18–21] suggests that the ground state has long-range magnetic order. However, making the interactions spatially anisotropic can lead to a very rich ground-state phase diagram.[22]

The spatially anisotropic model, defined by a nearest-neighbor exchange constant J_1 along one axis and J_2 along all other axes (see Fig. 1), interpolates between the limits of square-lattice ($J_1=0$), triangular-lattice ($J_2=J_1$), and decoupled linear chain ($J_2=0$) limits.[23,24] It has been studied by spin-wave theory,[25] series expansions,[22] large-N techniques,[26] slave fermions,[27] Schwinger bosons with Gaussian fluctuations,[28] and variational quantum Monte Carlo techniques.[29] Quantum fluctuations are largest for $J_1 \simeq 0.8J_2$ and for $J_1 > 4J_2$,[22,25] and so for these parameter regions one is most likely to observe quantum disordered phases.

From an experimental point of view, it is highly desirable to have a definitive way to determine the values of the exchange parameters for individual material systems. Recently, it has been shown how for materials with relatively small

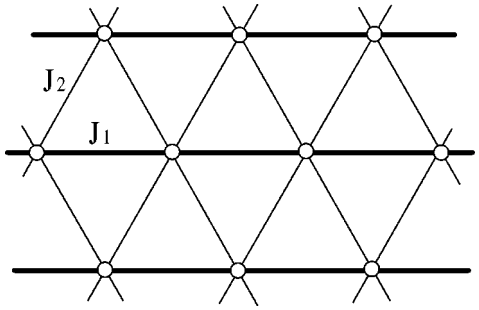

FIG. 1. The spatially anisotropic exchange constants for the Heisenberg model on the triangular lattice. The model can also be viewed as a square lattice with an extra exchange along one diagonal.

values for the Heisenberg exchange constants J this can be done in high magnetic fields, using inelastic neutron scattering to measure the spin-wave dispersion in the field induced ferromagnetic phase.[30] The temperature dependence of the magnetic susceptibility is one of the most common experimental measurements and it would be very useful if that can be used to determine the extent of frustration and the various exchange constants directly. It is particularly important to have a scheme for materials, where the very high-temperature behavior of the system ($T \gg J$) is not accesible to experiments. Previously, Castilla, Chakravarty, and Emery pointed out how the temperature dependence of the magnetic susceptibility of the antiferromagnetic spin chain compound $CuGeO_3$ implied significant magnetic frustration.[31] In that case, it constrains the ratio of the nearest- and next-nearest-neighbor exchanges along the chain.[32] Similarly, it is reasonable to expect that the temperature dependence of the magnetic susceptibility should depend on frustration in two-dimensional models also and hence constrain the ratio J_1/J_2.

The Mott insulating phase of the organic molecular crystals is of particular interest because under pressure the materials considered become superconducting. A possible RVB theory of superconductivity in such materials, emphasizing the role of frustration, has recently been proposed.[33] These materials have exchange constants in the range of several hundred K, and their behavior has led to several puzzles. Tamura and Kato[34] measured the temperature dependence of the magnetic susceptibility for five organic molecular crystals in the family β'-$[Pd(dmit)_2]X$ (where dmit is the electron acceptor molecule thiol-2-thione-4, 5-dithiolate, C_3S_5) and the cation $X = Me_4As$, Me_4P, Me_4Sb, Et_2Me_2P, and Et_2Me_2Sb, where $Me = CH_3$ and $Et = C_2H_5$, denote methyl and ethyl groups, respectively). They compared their results with the predictions for the square and triangular lattices and found that for all the materials the results could be fitted by the high-temperature series expansion for the triangular lattice. However, some and not all of them undergo a transition to a magnetically ordered state at low temperatures.

Recently, Shimizu *et al.*[35] showed using ^1H nuclear magnetic resonance that κ-$(BEDT\text{-}TTF)_2Cu_2(CN)_3$ did not undergo magnetic ordering and that the temperature dependence of the uniform magnetic susceptibility could still be fit by that for the triangular lattice. However, it should be stressed that for these molecular crystals the underlying triangular lattice of molecular dimers (to which each spin is associated) is not isotropic,[12] and so it is important to know the extent of the spatial anisotropy because this has a significant effect on the possible ground state. The isotropic triangular lattice is believed to be ordered, but for $J_1/J_2 = 0.7$–0.9 the anisotropic lattice could be quantum disordered.[22] Hence determination of the actual ratio is important for understanding these materials.

Here, we use high-temperature series expansions to calculate the temperature-dependent uniform susceptibility of the spatially anisotropic triangular-lattice models. Such calculations have been done previously for the pure square- and triangular-lattice cases[36,37] but not for the spatially anisotropic triangular-lattice model. This method is particularly useful here, as it allows one to cover the full range of J_1/J_2 ratios at once. Our main finding is that the susceptibility, for these antiferromagnets, shows a broad maximum at a temperature (which we call the peak temperature T_p) of order the Curie-Weiss temperature. If the exchange constants are scaled to give the same peak location, the magnitude of the peak susceptibility varies with frustration. The unfrustrated models, represented by the square-lattice and the linear-chain limits have similar peak susceptibilities. The triangular-lattice deviates the most from them, having a much smaller peak value, and a much flatter temperature dependence. The parameter regimes, where the ground states could be spin disordered, do not stand out in these calculations[22] and are similar to the triangular-lattice limit. The reason for this is probably that at the temperature scales considered the susceptibility is largely determined by short-range frustration, rather than long-length scale physics such as the existence of spin liquid states at zero temperature.

Comparison with the measured susceptibility of Cs_2CuCl_4 and Cs_2CuBr_4 leads to exchange parameters in agreement with previous neutron measurements. For the organic materials, it shows that they are all close to the isotropic triangular-lattice limit. But, some of them could be weakly anisotropic, leading to a quantum-disordered ground state. Since the organic materials are close to a Mott metal-insulator transition, we consider the possible role of multiple-spin exchange. Such interactions can be necessary for a quantitative description of such materials.[38]

II. FRUSTRATED MODEL

The spatially anisotropic triangular lattice is shown in Fig. 1. The antiferromagnetic Heisenberg model is described by the Hamiltonian

$$H = J_1 \sum_{a} \mathbf{S}_i \cdot \mathbf{S}_j + J_2 \sum_{b} \mathbf{S}_i \cdot \mathbf{S}_j, \tag{1}$$

where the first sum runs over all nearest-neighbor pairs along the x axis and the second sum runs over all other nearest-neighbor pairs. The vectors $\mathbf{S}$ represent spin-$1/2$ operators. It is evident that, for $J_1 = 0$, the model is equivalent to the square-lattice Heisenberg model, for $J_2 = J_1$ it is equivalent to the isotropic triangular lattice model, and in the limit $J_2 \to 0$, it is equivalent to a model of decoupled linear chains.

We now discuss how we might quantify how the amount of frustration in the model varies with J_2/J_1. Possible measures of frustration which have been discussed before include:

(i) The number of degenerate ground states.

(ii) How the competing interactions prevent the pairwise collinear alignment of spins that would give neighboring spins the lowest interaction energy.

In order to quantify (ii), Lacorre[39] considered classical spins and introduced a "constraint" function $F_c = -E_0/E_b$ which is the ratio of the ground-state energy E_0 of the system to the "base energy" E_b which is the sum of all bond energies if they are independently fully satisfied, i.e.,

$$E_b = -\sum_{ij} |J_{ij}| (\mathbf{S}_i \cdot \mathbf{S}_j)_{\max}. \tag{2}$$

Lacorre suggested that F_c has values ranging from -1 (no frustration) to $+1$ (complete frustration). However, for spin

models that have a traceless Hamiltonian the ground-state energy cannot become positive. So, F_c must lie between -1 (unfrustrated) and 0 (fully frustrated)—the largest possible value of F_c is zero. Considering a single isosceles triangular plaquette taken from the lattice in Fig. 1, Lacorre found that for classical (large-S) spins as a function of J_2/J_1, F_c had its maximum value $(-1/2)$ for the isotropic triangle $(J_1=J_2)$. The same result holds for the infinite lattice.

Kahn[40] recently stressed that for Heisenberg spins the degeneracy of the ground state depends on the value of the spin quantum number S as well as the geometry of the plaquette. For example, on an isotropic triangle, the ground state is fourfold degenerate for $S=1/2$ but nondegenerate for $S=1$.[41] On a single isosceles triangle, for $S=1/2$, the ground state has total spin $S_T=1/2$ and is twofold degenerate for $J_1\neq J_2$ and fourfold degenerate at the isotropic point $J_1=J_2$. We find that both F_c is maximal $(-1/3)$ and the ground state has the highest degeneracy for $J_1=J_2$. On the other hand, for spin $S=1$ the ground state is a nondegenerate singlet $(S_T=0)$ for a wide region near the isotropic limit $(0.5<J_1/J_2<2)$, is threefold degenerate $(S_T=1)$ outside this range $(J_1/J_2<0.5$ or $J_1/J_2>2)$ and has accidental fourfold degeneracy at the special points $J_1/J_2=0.5,2$. The function F_c has no singular maximum, but a plateau at -0.5 for the whole range $0.5<J_1/J_2<2$, so the spin-1 case is much less frustrated than the extreme spin-$1/2$ case.

The above properties of the degeneracy and constraint function are not unique to quantum spins but also hold for the Ising model on the same lattice. For a single isosceles triangle and for $S=1/2$ the ground-state energy changes at $J_1=J_2$ from $-J_1/4$ for $J_1>J_2$, to $(-2J_2+J_1)/4$ for $J_1<J_2$. The base energy is $E_b=-(J_1+2J_2)/4$ and hence F_c has its maximum value $(-1/3)$ when $J_1=J_2$. The degeneracy of the ground state is 2 (only up-down symmetry) for $J_1<J_2$, 6 (only all up and all down are not ground states) for $J_1=J_2$, and 4 (either one of the J_2 bonds can be dissatisfied) for $J_1>J_2$. So indeed by both measures for $J_1=J_2$ the model on a triangle is most frustrated. Extending this analysis for a single triangle to a large lattice of N sites the difference is even more dramatic as the degeneracy is[9] $\exp(cN)$ for $J_1=J_2$, and is easily seen to be only 2 for $J_1<J_2$ and $\exp(c'N^{1/2})$ for $J_1>J_2$, where c, c' are numbers of order 1. So the model has the largest ground-state degeneracy at the isotropic point.

Although this paper is concerned with the quantum spin model, the reason we mention the above properties of classical models is because an important question is whether our results concerning the connection between the amount of frustration and the temperature dependence of the susceptibility are also exhibited by the corresponding classical Heisenberg and Ising models. This may be the case if the temperature dependence of the susceptibility down to the peak is largely determined by the frustration and correlations associated with a single placquette.

With regard to measures of frustration we also note from an experimental point of view two measures that have been proposed previously.[6] (i) The ratio of the Curie-Weiss temperature to the magnetic ordering temperature. This increases with increasing frustration. (ii) The amount of entropy at temperature scales much less than the exchange energy.

III. HIGH-TEMPERATURE SERIES EXPANSIONS

The high-temperature series expansion method has been extensively applied to and tested for quantum lattice models.[42] We have obtained high-temperature expansions for arbitrary ratio of J_1/J_2 to order β^{10}. We express the uniform susceptibility, per mole, as

$$\chi=\frac{N_A g^2\mu_B^2}{kT}\bar{\chi}, \tag{3}$$

where N_A is Avogadro's number, g the g factor, μ_B a Bohr magneton, k the Boltzmann constant, and T the absolute temperature. The dimensionless quantity $\bar{\chi}$ can be expressed in a high-temperature expansion in J_2/T and $y=J_1/J_2$, as

$$\bar{\chi}=\sum_{n=0}(J_2/T)^n\sum_{m=0}^{n}c_{m,n}y^m/(4^{n+1}n!). \tag{4}$$

The integer coefficients $c_{m,n}$ complete to order $n=10$ are presented in Table I.

IV. CURIE-WEISS BEHAVIOR AND BEYOND: SERIES EXTRAPOLATIONS

As is well known, the high-temperature behavior of the susceptibility, per mole, is given by a Curie-Weiss law

$$\chi=\frac{C}{T+T_{\mathrm{cw}}}. \tag{5}$$

For our model, the Curie constant

$$C=N_A g^2\mu_B^2/4k=Ag^2, \tag{6}$$

with $A=0.0938$ in cgs units. The Curie-Weiss temperature is

$$T_{\mathrm{cw}}=J_2+J_1/2. \tag{7}$$

From an experimental point of view, an important question is: How low in temperature is the Curie-Weiss law valid? To investigate this, we plot in Fig. 2(a), the normalized inverse susceptibility as a function of T/T_{cw} for several parameters, together with the Curie-Weiss law. It is clear that below $T<10T_{\mathrm{cw}}$, the Curie-Weiss fit is no longer accurate. Deviations from the Curie-Weiss behavior are the smallest near the triangular-lattice limit, and largest for linear chains. If one were to fit the inverse susceptibility below some temperature to a Curie-Weiss behavior, one would get a systematically larger Curie-Weiss temperature. To quantify this, we define an effective temperature-dependent Curie-Weiss constant $T_{\mathrm{cw}}^{\mathrm{eff}}$ as

$$T_{\mathrm{cw}}^{\mathrm{eff}}=-T-\frac{\chi}{d\chi/dT}. \tag{8}$$

If one was to fit χ^{-1} to a linear curve in the vicinity of some temperature (T) and use the intercept to estimate the Curie-Weiss constant, one would get $T_{\mathrm{cw}}^{\mathrm{eff}}$. Figure 2(b) shows how

TABLE I. Series coefficients for the high-temperature expansions of the uniform susceptibility $\bar{\chi}$ in Eq. (4). Nonzero coefficients $c_{m,n}$ up to order $n=10$ are listed.

(m,n)	$c_{m,n}$	(m,n)	$c_{m,n}$	(m,n)	$c_{m,n}$	(m,n)	$c_{m,n}$
(0,0)	1	(3,5)	−7680	(7,7)	20480	(7,9)	−129328128
(0,1)	−4	(4,5)	1920	(0,8)	4205056	(8,9)	−159694848
(1,1)	−2	(5,5)	−672	(1,8)	−58877952	(9,9)	19133440
(0,2)	16	(0,6)	23488	(2,8)	110985216	(0,10)	−2574439424
(1,2)	32	(1,6)	293376	(3,8)	−501760	(1,10)	52032471040
(0,3)	−64	(2,6)	111552	(4,8)	101972480	(2,10)	−735774720
(1,3)	−264	(3,6)	411392	(5,8)	−84013056	(3,10)	−29924454400
(2,3)	−96	(4,6)	−115968	(6,8)	29817856	(4,10)	15318384640
(3,3)	16	(5,6)	70656	(7,8)	−15618048	(5,10)	38033190912
(0,4)	416	(6,6)	−12768	(8,8)	2923776	(6,10)	−40192143360
(1,4)	1216	(0,7)	207616	(0,9)	−198295552	(7,10)	48646737920
(2,4)	2400	(1,7)	−1766016	(1,9)	−571327488	(8,10)	−13533921280
(3,4)	−512	(2,7)	−7739648	(2,9)	3934844928	(9,10)	4594278400
(4,4)	80	(3,7)	−1804992	(3,9)	−4115195904	(10,10)	−869608960
(0,5)	−4544	(4,7)	−3373440	(4,9)	3772164096		
(1,5)	−10880	(5,7)	689920	(5,9)	−1888413696		
(2,5)	−20480	(6,7)	120064	(6,9)	1134317568		

$T_{\mathrm{cw}}^{\mathrm{eff}}$ varies with temperature for several parameter ratios. It shows that attempts to fit to a Curie-Weiss behavior below four times the Curie-Weiss temperature can result in an overestimate in the Curie-Weiss constant by less than 20% for the isotropic triangular lattice, whereas for the square lattice an error of 40% is possible. Similar observations were made previously for the classical Heisenberg antiferromagnet on a *kagomé* lattice.[43]

To obtain the susceptibility for $T \leqslant T_{\mathrm{cw}}$, we need to develop a series extrapolation scheme. We have used *d*-log Padé and the integral differential approximants to extrapolate the series.[44–46] For the linear chain model we use the very long series given by Takahashi[47] and for the square- and triangular-lattice cases we have also used the longer series.[36,37] In the former case, the calculated susceptibility agrees well with the exact results obtained from thermodynamic Bethe-ansatz calculations.[48] For the square- and triangular-lattice cases it also agrees well with previous numerical calculations.[36,49] In all cases, several integral/*d*-log-Pade approximants are calculated, and in the plots below two outer approximants are shown, i.e., a large number of approximants lie between those shown. Based on our general experience with series extrapolations,[50] we feel confident that as long as the upper and lower curves are not too far from each other, they bracket the true value of the thermodynamic susceptibility. In general, we find that the extrapolations work well down to the peak temperature and begin to deviate from each other below the peak. It is not possible to address the zero- and very low-temperature behavior of the susceptibility from these calculations.

In Fig. 3, we show the uniform susceptibility, for different $y=J_1/J_2$, as a function of temperature. For all J_1/J_2 ratios, there are two plots showing the upper and lower limits of extrapolated values as discussed in the previous paragraph. The susceptibility is scaled to have a peak value of unity, and the temperature axis is scaled by the peak susceptibility to a dimensionless relative temperature. One finds that the susceptibility peaks at a comparable relative temperature for the unfrustrated square-lattice and linear chains. The primary difference between these two models lies in the behavior of the susceptibility below the peak. It decreases much more slowly for the linear chains than it does for the square lattice. We believe that this is related to the fact that longer-range antiferromagnetic correlations grow much faster for the square lattice than they do for linear chains. Thus the shift of the spectral weight away from zero wave vector occurs more gradually for linear chains. For the triangular lattice, the peak is shifted to much lower relative temperatures. Note that the triangular lattice has a peak at a temperature even lower than for $J_1/J_2=0.8$, where $T=0$ calculations show an absence of long-range order.[22]

From Fig. 3 it is clear that frustration leads to a reduction in the magnitude of the product $\chi_p T_p$ as well as a reduction in the peak temperature T_p with respect to the Curie-Weiss temperature T_{cw}. These parameters are plotted in appropriate dimensionless units in Fig. 4 as a function of the frustration ratio $J_1/(J_1+J_2)$, and both have a minimum around the triangular-lattice limit $J_1=J_2$. To connect with experiments we also show the ratio of the peak temperature T_p and the Zeeman energy required to fully polarize the spins $g\mu_B B_{\mathrm{sat}}$, related to the couplings strength by[30]

$$g\mu_B B_{\mathrm{sat}} = \begin{cases} 2J_1 + 2J_2 + \dfrac{J_2^2}{2J_1} & \text{for } J_2 \leqslant 2J_1 \\ 4J_2 & \text{for } J_2 \geqslant 2J_1. \end{cases} \tag{9}$$

Figure 4 also shows the ratio $\chi(4T_p)/\chi_p$, which is a measure of the flatness of the curves on the high-temperature side of

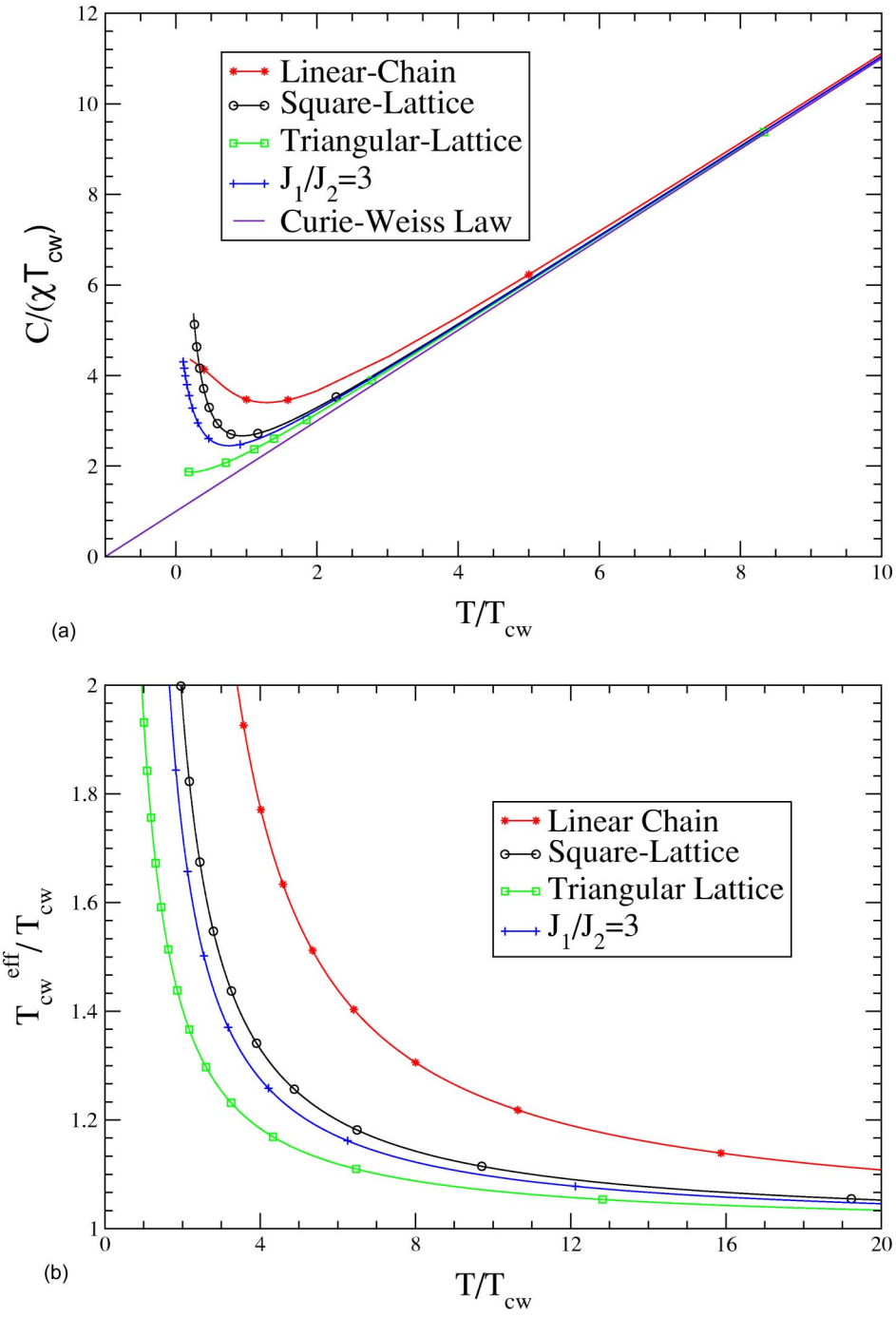

FIG. 2. (Color online) (a) Inverse magnetic susceptibility as a function of temperature in relative units of the Curie-Weiss constant T_{cw}. The susceptibility departs from the high-temperature Curie-Weiss limit [Eq. (4)] already at temperatures a few times T_{cw} due to short-range correlations. The smallest departure occurs for the triangular lattice. (b) Effective Curie-Weiss constant T_{cw}^{eff} vs temperature found by a local fit of the susceptibility to the Curie-Weiss form, Eq. (7). The plot shows that fitting data below $4T_{cw}$ can result in large overestimates of the Curie-Weiss constant.

the peak. A larger value of this ratio implies a slower decay of the susceptibility with temperature. These quantities clearly show that the triangular lattice is the most frustrated, with the lowest peak temperature relative to the scale of the exchange interactions, T_p/T_{cw} or $kT_p/g\mu_B B_{sat}$, the smallest dimensionless ratio $T_p\chi_p$ and the flattest peak denoted by the largest $\chi(4T_p)/\chi_p$. The plots look very symmetrical around the triangular-lattice limit, and there is nothing anomalous about the case of $J_1/J_2=0.8$, where zero-temperature studies give a disordered and gapped dimerized ground state.[22] We note that all of the extracted parameters in Fig. 4 are from the susceptibility curve at temperatures above the peak and in order to see evidence for the presence of a gap for $J_1/J_2 \sim 0.8$ as opposed to no gap in the isotropic triangular-lattice case one would be required to analyze the susceptibility curve at temperatures much below the estimated gap $\Delta \sim 0.25J_2 \sim 0.5T_p$ in the dimerized state,[22] and such low temperatures are not accessible by the present series calculations.

V. COMPARISON WITH EXPERIMENTAL SYSTEMS

In this section, we compare our theoretical results with experimental data on Cs_2CuCl_4, Cs_2CuBr_4, and various or-

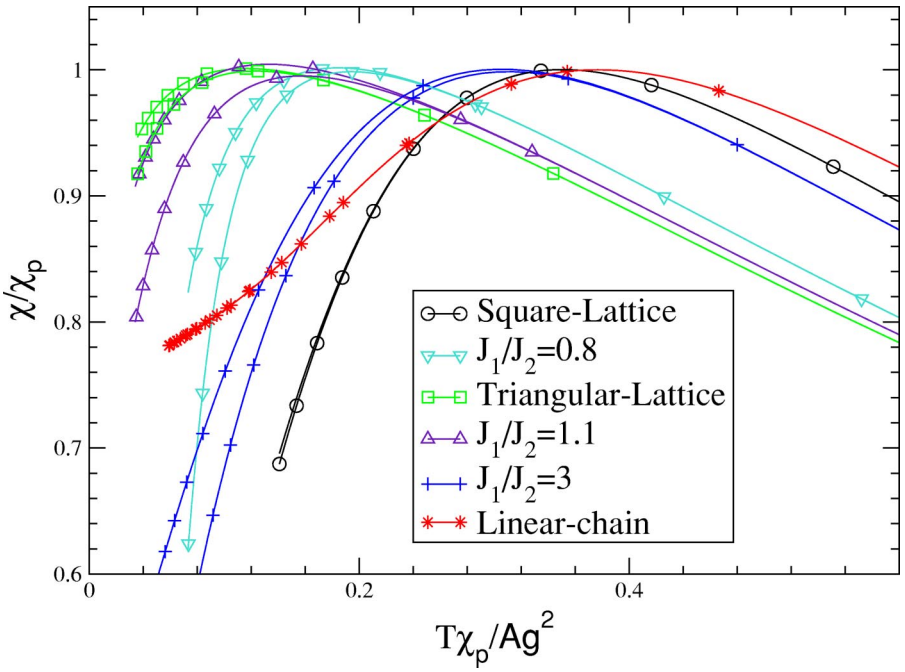

FIG. 3. (Color online) Susceptibility vs temperature for different values of J_1/J_2. The peak susceptibility χ_p and the Curie-Weiss constant $C=Ag^2$ are used to define a dimensionless relative temperature scale. As discussed in the text, the two curves shown for each J_1/J_2 value are due to different extrapolation schemes. For the most frustrated triangular lattice the peak in the susceptibility occurs at the lowest relative temperature.

ganic materials. In Fig. 5, we show the susceptibility as a function of temperature for different J_1/J_2 ratio, where the temperature is scaled by the peak temperature (T_p) and the susceptibility itself is scaled by the peak temperature to give a dimensionless reduced susceptibility. This plot is very instructive as it allows one to clearly read out the J_1/J_2 ratios. Also shown are the susceptibilities for the materials Cs_2CuCl_4 and Cs_2CuBr_4, with their g values taken from electron spin resonance experiments.[52,53] In this plot with no free parameters, it is apparent that the J_1/J_2 ratio is near 3.0 for Cs_2CuCl_4 and near 2.0 for Cs_2CuBr_4. Some of these results can also be seen from Fig. 4, where key dimensionless ratios of the temperature-dependent susceptibility are shown.

A more detailed comparison of the susceptibility for the materials, Cs_2CuCl_4 and Cs_2CuBr_4, allowing g to vary freely is shown in Fig. 6. Once g is allowed to vary, the material Cs_2CuCl_4 can be fit above the peak not too badly even with the pure square-lattice model (not shown). However, a much improved fit happens with $J_1/J_2=3$ and $J_2=1.49$ K in excellent agreement with the exchange values extracted directly from neutron-scattering measurements.[30] Also shown are fits to linear chain and triangular-lattice limits, which bracket $J_1/J_2=3$. One can see significant deviation in both limits. The large deviation from the isotropic triangular-lattice case shows that frustration is relatively weak in this material.

For Cs_2CuBr_4, the best fit for $J_1/J_2=2$ arises with $J_2=6.99$ K. However, when g is allowed to vary, a range of J_1/J_2 values from 1.8 to 2.8 give comparable fits, several of which are shown in figure. In general, the high-temperature data are better fit by a larger J_1/J_2 value, whereas the data at and around the peak are better fit by a smaller J_1/J_2 value. No choice of parameters can fit the very low-temperature data (below half the peak temperature). These values are also consistent with previous estimates. Using the value of the incommensurate ordering wave vector $\mathbf{Q}=0.575(1)\mathbf{b}^*$ observed by neutron scattering,[11] classical spin-wave theory

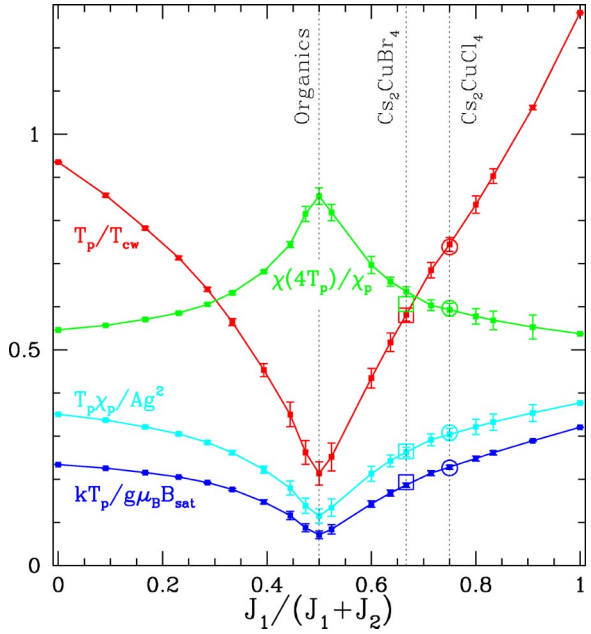

FIG. 4. (Color online) Variation of the key parameters of the susceptibility curve $\chi(T)$ as a function of the frustration ratio $J_1/(J_1+J_2)$: location of peak temperature T_p relative to the overall energy scale of the couplings, given by the Curie-Weiss constant T_{cw} or the saturation field B_{sat} required to overcome all antiferromagnetic interactions (see text for more details), dimensionless product of peak susceptibility and peak temperature $T_p\chi_p/Ag^2$ (with $A=0.0938$ in cgs units), and flatness of the susceptibility curve $\chi(4T_p)/\chi(T_p)$. The isotropic triangular lattice ($J_1=J_2$) is the most frustrated with the lowest relative peak temperature T_p/T_{cw}, lowest peak susceptibility, and flattest curve at temperatures above the peak. The circles are values extracted from the experimental data for Cs_2CuCl_4 from Ref. 51 and the squares are for Cs_2CuBr_4 (Ref. 11). This suggests that the ratio J_1/J_2 is close to 3.0 and 2.0, respectively, for these two materials. The former is consistent with independent estimates from neutron scattering (Ref. 30).

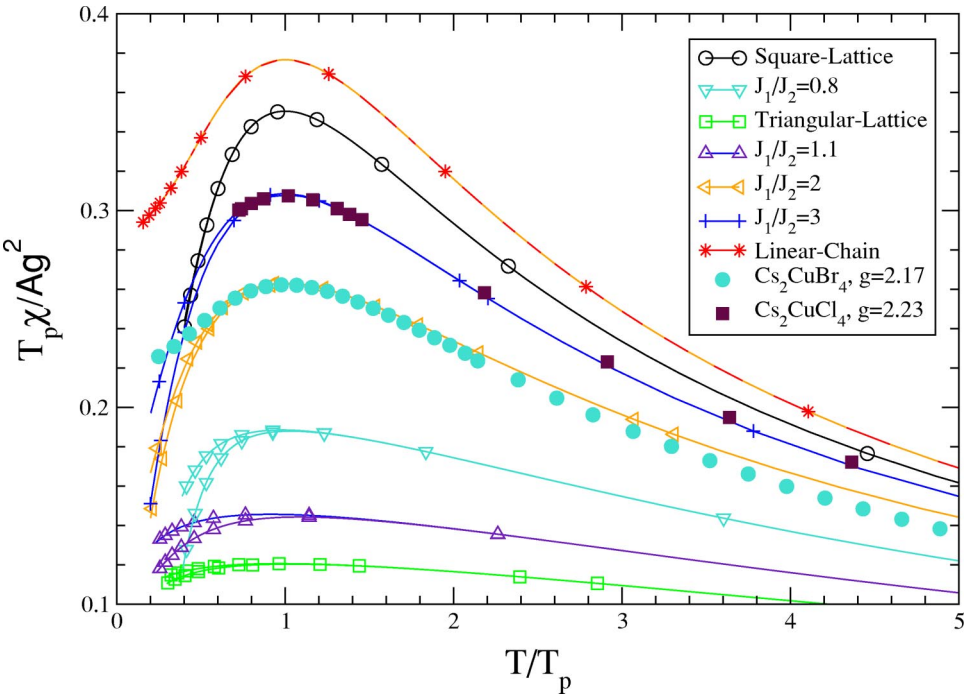

FIG. 5. (Color online) Susceptibility vs temperature in units of the peak temperature T_p. The isotropic triangular lattice (green line) has the lowest and flattest susceptibility. Solid squares show data points for the anisotropic triangular lattice material Cs_2CuCl_4 (a axis, Ref. 51), solid circles show data for Cs_2CuBr_4 from Ref. 11.

gives $J_1/J_2=2.14$ whereas including quantum renormalization corrections as predicted by large-N Sp(N) theory[26] gives $J_1/J_2\sim 1.8$, and series expansions[22] gives $J_1/J_2\sim 1.4$. This calls into question the rather large renormalization of the ordering wave vector found in the series expansion study.

Now we turn to the organic materials. In Fig. 7, we show a corresponding comparison for the material κ-(BEDT-TTF)$_2$Cu$_2$(CN)$_3$. Only the theoretical data for the isotropic triangular lattice are shown. One can see an important difficulty in using the T_p-scaled plots near the triangular-lattice limit to determine J_1/J_2. For the organic material, κ-(BEDT-TTF)$_2$Cu$_2$(CN)$_3$, the measured susceptibility is very flat and it is difficult to determine the peak temperature T_p. From the data, the peak temperature appears to be between 65 and 95 K. Using the values for T_p of 65 and 95 K, one can either get the data to fall above or below the triangular-lattice values. A suitably chosen peak temperature allows one to get very close agreement with the triangular-lattice limit. This peak temperature can also be used to determine the exchange constant. However, for the triangular lattice, there is theoretical uncertainty in the peak location. Hence it is more accurate to directly fit the experimental data to theory to obtain the exchange constants. For κ-(BEDT-TTF)$_2$Cu$_2$(CN)$_3$, fixing $g=2.006$ and $J_1=J_2$, the best fit leads to $J_1=256$ K, a value close to that obtained by Shimizu *et al.*[35]

The ability to fit flat susceptibilities to the isotropic triangular-lattice model is further illustrated in Fig. 8, where the susceptibility data are shown from five different molecular crystals in the family β'-[Pd(dmit)$_2$]X (where dmit is the electron acceptor molecule thiol-2-thione-4, 5-dithiolate, C_3S_5) and the cation X=Me$_4$As, Me$_4$P, Me$_4$Sb, Et$_2$Me$_2$P, and Et$_2$Me$_2$Sb, where Me=CH$_3$ and Et=C$_2$H$_5$, denote methyl and ethyl groups, respectively). We have taken the g value to be 2.04. By adjusting the peak temperature, they can all be brought to rough agreement with the triangular-lattice model. Assuming isotropic interactions, and $g=2.04$, we estimate the exchange constants to be 283, 289, 270, 279, and 247 K, respectively. It is clear that none of these organic materials are far from the isotropic triangular-lattice limit. But, we emphasize that by this method it is difficult to discriminate between J_1/J_2 ratios in the range $0.85<J_1/J_2<1.15$. Note that the latter regions also include quantum disordered phases.

To avoid the problem of determining the peak temperature, we go back to Fig. 3, and scale the data by the peak susceptibility. These can be inferred accurately from the data, even when the peak temperature cannot. In Fig. 9, we show such a comparison of experimental data with theory. The data for κ-(BEDT-TTF)$_2$Cu$_2$(CN)$_3$ lie extremely close to the isotropic triangular-lattice case. The other materials deviate from the $J_1=J_2$ limit, but still lie in the range $0.85<J_1/J_2<1.15$. If we assume that the systems are described by the isotropic triangular lattice, the exchange constant can be read of from the peak susceptibility by using the relation $J=0.0035g^2/\chi_p$. This leads to exchange constants of 250 K for κ-(BEDT-TTF)$_2$Cu$_2$(CN)$_3$ and 280, 289, 260, 273, and 236 K for the other materials. These values are close to those obtained from the best fits.

It should be noted here that in the experimental data, a Curie term from magnetic impurities and a diamagnetic term has been subtracted and these can also influence the determination of exchange parameters. However, it is unlikely that any of these materials are very far from the isotropic triangular-lattice limit.

From the fits the Heisenberg couplings are comparable for all materials and around 250 K. We now consider how these compare with quantum chemistry calculations. The exchange constants can be related to parameters in an underlying Hubbard model[12,34,54] where $J=2t^2/U$ and t is the intersite (i.e., interdimer) hopping and U is the cost of double occupancy

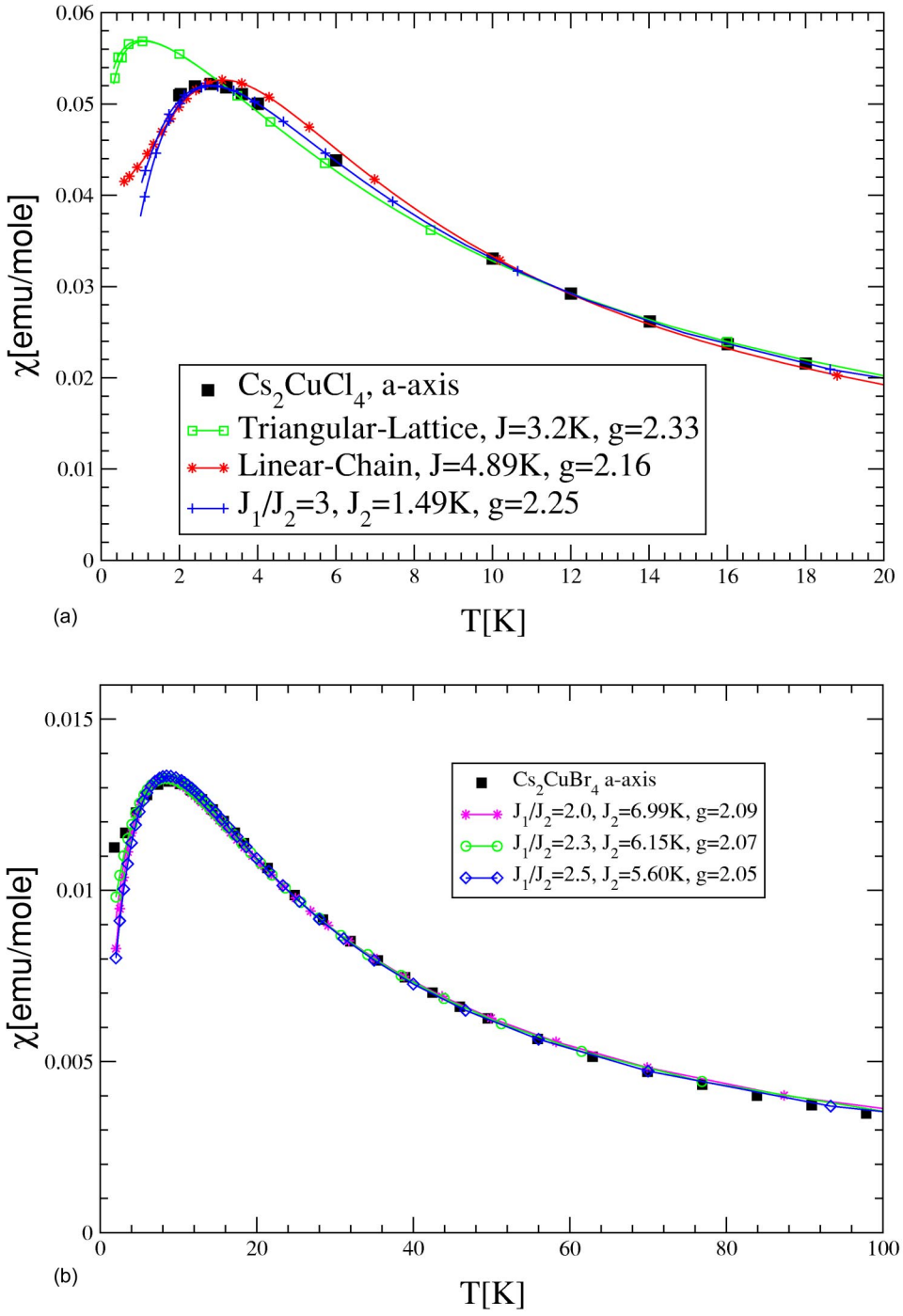

FIG. 6. (Color online) Fits of the susceptibility in Cs_2CuCl_4 (a) and Cs_2CuBr_4 (b), see text.

for two electrons or holes on a dimer. If the Coulomb repulsion U_0 on a single molecule within the dimer is much larger than the intermolecular hopping t_0 within a dimer then $U \simeq 2t_0$. For β'-[Pd(dmit)$_2$]X electronic structure calculations based on the local-density approximation (LDA) (Refs. 34, 54, and 55) give $t \sim 30$ meV and $t_0 \sim 500$ meV, and so $J \sim 50$ K. For κ-(BEDT-TTF)$_2$Cu$_2$(CN)$_3$ Hückel electronic structure calculations give $t \sim 50$ meV and $t_0 \sim 200$ meV.[56,57] The resulting $U \simeq 400$ meV is comparable to that deduced from measurements of the frequency-dependent optical conductivity of similar κ materials.[12,58] This value of U is smaller than values deduced from quantum chemistry calculations on isolated dimers, which do not take into account screening.[59] Using the above values of t and U gives $J \sim 100$ K.

Note that the quality of fit is best for the material κ-(BEDT-TTF)$_2$Cu$_2$(CN)$_3$, where it really fits well with the isotropic triangular-lattice model. However, it is also a system that does not order down to very low temperatures.[35] This remains a puzzle. The quality of fits was not as good for the other organic compounds. It is quite possible that the organics have other interactions not captured by the Heisenberg model. In a Mott insulator when a perturbation expansion in t/U is used to derive an effective Hamiltonian for the

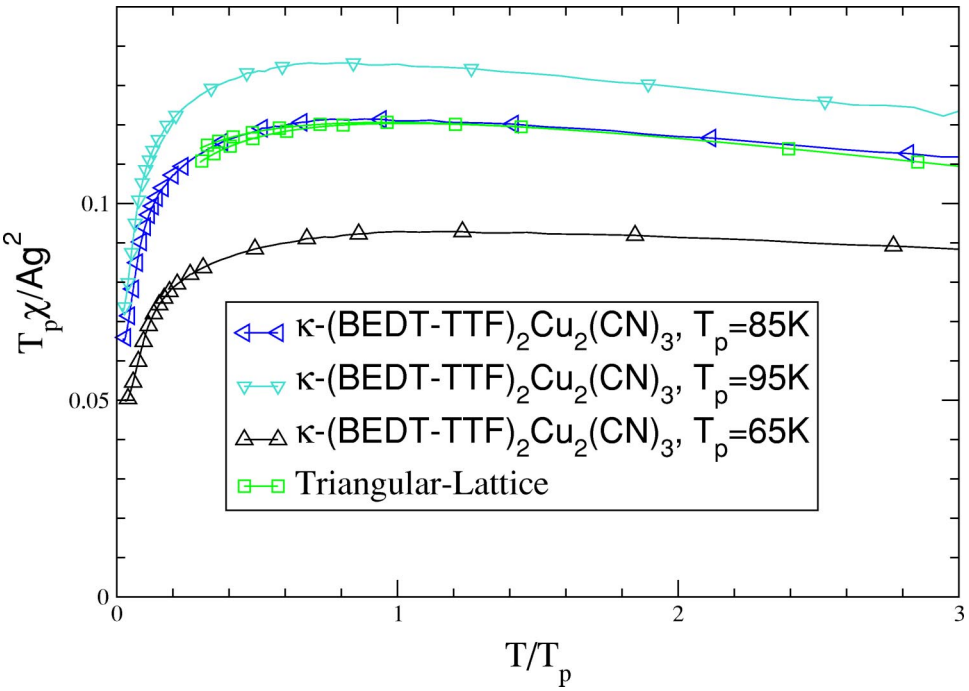

FIG. 7. (Color online) Comparison of the temperature dependence of the magnetic susceptibility of κ-(BEDT-TTF)$_2$Cu$_2$(CN)$_3$ with series expansions calculations for isotropic triangular lattice. The experimental data are from Ref. 35. A value of $g=2.006$ was used based on electronic spin resonance measurements (Ref. 56). We see that this material is well described by a Heisenberg model on the isotropic triangular lattice, with peak temperature $T_p=85$ K. Note also that the agreement is quite sensitive to changes in the value of T_p, a quantity that is difficult to pinpoint in a flat curve.

spin degrees of freedom one finds that to fourth order in t/U there are cyclic exchange terms in the Hamiltonian.[61] If $U/t<10$ then these terms may be important. Recent neutron-scattering studies showed the effect of such interactions on the dispersion of spin excitations in La_2CuO_4.[38]

The metallic phase of the organics are in the regime $U/t\sim 5$–10 (Ref. 12) and so one might expect multiple-exchange terms to be relevant in the insulating phase. For the triangular-lattice triple exchange is also possible. However, for spin-1/2 this just corresponds to a renormalization of the nearest-neighbor two-particle exchange.[62] The frustrating effects of multiple-spin exchange on the isotropic triangular lattice lead to rich physics and have an experimental realization in monolayers of solid ^{3}He on graphite.[63] Let J denote the nearest-neighbor exchange and J_4 the multiple spin exchange, involving the four spins comprising a pair of triangular plaquettes. This model has been studied extensively and exact diagonalization calculations suggest that the 120° Néel state, which is the ground state for $J_4=0$, is destroyed when $J_4>0.1J$.[64] It is appealing to think that this could be the explanation for why κ-(BEDT-TTF)$_2$Cu$_2$(CN)$_3$ does not magnetically order, whereas it should if it is really described by the isotropic triangular-lattice nearest-neighbor model. This material is close to a Mott-Hubbard metal-insulator

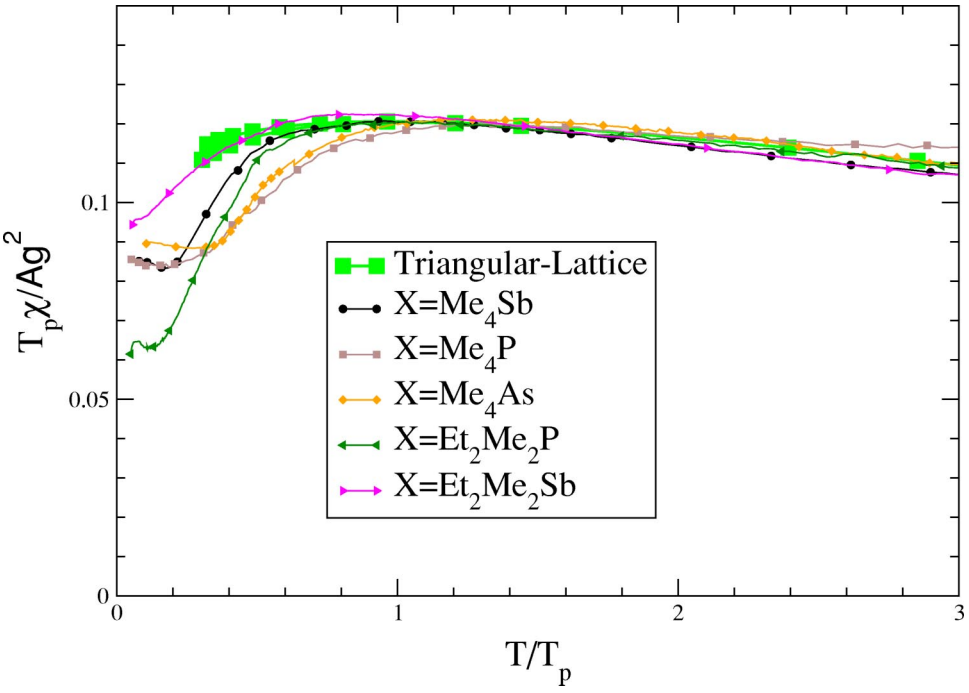

FIG. 8. (Color online) Comparison of the temperature dependence of the magnetic susceptibility of five different organic molecular crystals from the family β'-[Pd(dmit)$_2$]X (different X are indicated with Me=CH$_3$, Et=C$_2$H$_5$) with series expansions for isotropic triangular lattice. Experimental data are from Ref. 34. A value of $g=2.04$ was used based on electronic spin resonance measurements (Ref. 60). All of these materials are well described by a Heisenberg model close to that for the isotropic triangular lattice, assuming that ring-exchange interactions do not need to be taken into account.

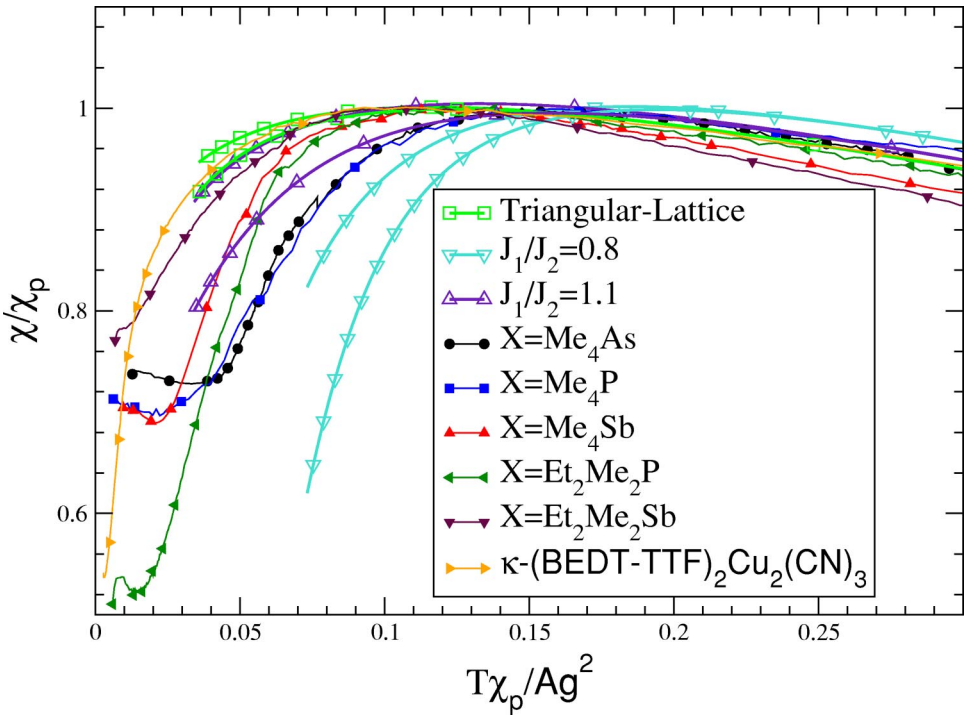

FIG. 9. (Color online) Parameter free comparison of the susceptibility data on organic materials with theoretical plots scaled by the peak susceptibility χ_p, which is easy to measure accurately for a flat curve. It is evident that the materials deviate only slightly from the isotropic triangular-lattice model and have J_1/J_2 ratios in the range 0.85–1.15.

transition since the insulating state is destroyed under pressure or uniaxial stress.[56,65] However, it is not clear that J_4 will be large enough in the actual material. The expressions derived from a t/U expansion give[61] $J_4/J=10(t/U)^2$. This means one must have $U<8t$ to obtain a spin liquid. However, exact diagonalization of the Hubbard model on the isotropic triangular lattice at half filling, shows that the insulating state only occurs for $U>12t$.[66] Hence it is not clear that multiple-spin exchange could account for the fact that this material appears to be close to the isotropic triangle but does not magnetically order. However, to definitively resolve this issue would require a detailed study of the spatially anisotropic model with four-spin exchange.

VI. CONCLUSIONS

In this paper, we have developed high-temperature expansions for the uniform susceptibility of the spatially anisotropic triangular-lattice Heisenberg model. We find that the temperature dependence of the susceptibility at temperatures of order the exchange constants are sensitive to frustration, that is, the ability of spins to align antiparallel to all their neighbors. The square-lattice and linear chain limits have similar reduced susceptibilities at and above the peak, while the triangular-lattice limit appears most frustrated, with the smallest and flattest susceptibilities. Comparison with various experimental systems shows that a variety of organic materials are close to the isotropic triangular-lattice limit, whereas the inorganic materials Cs_2CuCl_4 and Cs_2CuBr_4 are much less frustrated.

It would be nice to have a simple formalism which could provide an analytic relation between the peak susceptibility and exchange parameters. Qualitatively, our arguments show that short-range frustration, or the inability to align parallel with respect to neighbors as quantified by the parameter F_c in Sec. II, is maximum near the isotropic limit and this is what pushes the peak in the susceptibility down to lower temperatures. For a wide range of frustrated antiferromagnets it has been previously pointed out that the Curie-Weiss law holds to relatively low temperatures.[6,67] Several theoretical models, mostly for classical spins, have been developed to explain this.[68,69] Basically, frustration leads to individual plaquettes or spin clusters behaving essentially independently. However, our models are less frustrated than that and hence always develop substantial correlations. This means that any simplistic explanation is unlikely.

In organic molecular crystals a weak temperature dependence of the magnetic susceptibility is often interpreted as being evidence for metallic behavior, since for a Fermi liquid the susceptibility is weakly temperature dependent. However, this is inconsistent with the fact that in most of these materials above temperatures of about 50 K there is no Drude peak in the optical conductivity and the resistivity has a nonmonotonic temperature dependence and values of order the Mott limit.[12,70] This work shows that due to the substantial magnetic frustration the susceptibility can actually be due to local magnetic moments, even though in the range up to 300 K one does not see a clear Curie temperature dependence.

In a future study we will consider the temperature dependence of the specific-heat capacity for this model. A previous study[71] of the square lattice, single chain, and triangular-lattice Heisenberg model found that the peak in the specific heat versus temperature curve occurred around J for all models but was much broader for the triangular lattice. A related issue was that as the temperature decreases the entropy decreases much more slowly for the triangular lattice than the others.

Note added in proof. Recently, we became aware of other recent work by O. I. Motrunich[72] and S. S. Lee and P. A. Lee,[73] which also considered the possible role of multiple spin exchange in κ-(BEDT-TTF)$_2$Cu$_2$(CN)$_3$.

ACKNOWLEDGMENTS

We thank T. Ono, Y. Tokiwa, M. Tamura, and Y. Shimizu for sending us their experimental data. We thank R. Moessner and B. Powell for a critical reading of the manuscript. We have also benefitted from discussions with S. Bramwell, B. Powell, and D. McMorrow. This work was supported by the Australian Research Council (Z.W. and R.H.M.), US National Science Foundation Grant No. DMR-0240918 (R.R.P.S.), and United Kingdom Engineering and Physical Sciences Research Council Grant No. GR/R76714/01 (R.C.). R.H.M. thanks UC Davis, ISIS, Rutherford Appleton Laboratory, and the Clarendon Laboratory, Oxford University for hospitality. We are grateful for the computing resources provided by the Australian Partnership for Advanced Computing (APAC) National Facility and by the Australian Centre for Advanced Computing and Communications (AC3).

[1] G. Aeppli and P. Chandra, Science **275**, 177 (1997).
[2] T. Senthil, A. Vishwanath, L. Balents, S. Sachdev, and M. P. A. Fisher, Science **303**, 1490 (2004).
[3] For a review of quantum antiferromagnets in two dimensions, see G. Misguich and C. Lhuillier, in *Frustrated Spin Systems*, edited by H. T. Diep (World-Scientific, Singapore, 2003).
[4] J. E. Greedan, J. Mater. Chem. **11**, 37 (2001).
[5] For a review of frustrated magnets from a synthesis point of view, see A. Harrison, J. Phys.: Condens. Matter **16**, S553 (2004).
[6] A. P. Ramirez, Annu. Rev. Mater. Sci. **24**, 453 (1994).
[7] P. W. Anderson, Science **235**, 1196 (1987).
[8] P. W. Anderson, Mater. Res. Bull. **8**, 153 (1973); P. Fazekas and P. W. Anderson, Philos. Mag. **30**, 423 (1974).
[9] G. H. Wannier, Phys. Rev. **79**, 357 (1950).
[10] R. Coldea, D. A. Tennant, A. M. Tsvelik, and Z. Tylczynski, Phys. Rev. Lett. **86**, 1335 (2001); R. Coldea, D. A. Tennant, and Z. Tylczynski, Phys. Rev. B **68**, 134424 (2003).
[11] T. Ono, H. Tanaka, H. Aruga Katori, F. Ishikawa, H. Mitamura, and T. Goto, Phys. Rev. B **67**, 104431 (2003).
[12] R. H. McKenzie, Comments Condens. Matter Phys. **18**, 309 (1998).
[13] S. J. Clarke, A. J. Fowkes, A. Harrison, R. M. Ibberson, and M. J. Rosseinsky, Chem. Mater. **10**, 372 (1998).
[14] M. Suzuki, I. S. Suzuki, C. R. Burr, D. G. Wiesler, N. Rosov, and K. Koga, Phys. Rev. B **50**, 9188 (1994).
[15] S. T. Bramwell, S. G. Carling, C. J. Harding, K. D. M. Harris, B. M. Kariuki, L. Nixon, and I. P. Parkin, J. Phys.: Condens. Matter **8**, L123 (1996).
[16] V. Kalmeyer and R. B. Laughlin, Phys. Rev. Lett. **59**, 2095 (1987).
[17] R. Moessner and S. L. Sondhi, Phys. Rev. Lett. **86**, 1881 (2001).
[18] B. Bernu, P. Lecheminant, C. Lhuillier, and L. Pierre, Phys. Rev. B **50**, 10 048 (1994).
[19] R. R. P. Singh and D. A. Huse, Phys. Rev. Lett. **68**, 1766 (1992).
[20] D. J. J. Farnell, R. F. Bishop, and K. A. Gernoth, Phys. Rev. B **63**, 220402 (2001).
[21] L. Capriotti, A. E. Trumper, and S. Sorella, Phys. Rev. Lett. **82**, 3899 (1999).
[22] W. Zheng, R. H. McKenzie, and R. R. P. Singh, Phys. Rev. B **59**, 14 367 (1999).
[23] The classical version of this model was studied in H. Kawamura, Prog. Theor. Phys. Suppl. **101**, 545 (1990); W. Zhang, W. M. Saslow, and M. Gabay, Phys. Rev. B **44**, 5129 (1991).
[24] The thermodynamic properties of the Ising version of this model were found exactly by R. M. F. Houtappel, Physica (Amsterdam) **16**, 425 (1950). The exact correlation functions were found and analyzed extensively by J. Stephenson, J. Math. Phys. **5**, 1009 (1964); **11**, 420 (1970).
[25] A. E. Trumper, Phys. Rev. B **60**, 2987 (1999); J. Merino, R. H. McKenzie, J. B. Marston, and C.-H. Chung, J. Phys.: Condens. Matter **11**, 2965 (1999); M. Y. Veillette, J. T. Chalker, and R. Coldea, cond-mat/0501347 (unpublished).
[26] C.-H. Chung, J. B. Marston, and R. H. McKenzie, J. Phys.: Condens. Matter **13**, 5159 (2001); C.-H. Chung, K. Voelker, and Y. B. Kim, Phys. Rev. B **68**, 094412 (2003).
[27] Y. Zhou and X.-G. Wen, cond-mat/0210662 (unpublished).
[28] L. O. Manuel and H. A. Ceccatto, Phys. Rev. B **60**, 9489 (1999).
[29] S. Yunoki and S. Sorella, Phys. Rev. Lett. **92**, 157003 (2004).
[30] R. Coldea, D. A. Tennant, K. Habicht, P. Smeibidl, C. Wolters, and Z. Tylczynski, Phys. Rev. Lett. **88**, 137203 (2002).
[31] G. Castilla, S. Chakravarty, and V. J. Emery, Phys. Rev. Lett. **75**, 1823 (1995).
[32] For a detailed discussion, see K. Fabricius, A. Klumper, U. Low, B. Bochner, T. Lorenz, G. Dhalenne, and A. Revcolevschi, Phys. Rev. B **57**, 1102 (1998); A. Buhler, U. Low, and G. S. Uhrig, *ibid.* **64**, 024428 (2001).
[33] J. Y. Gan, Yan Chen, Z. B. Su, and F. C. Zhang, Phys. Rev. Lett. **94**, 067005 (2005); B. J. Powell and R. H. McKenzie, *ibid.* **94**, 047004 (2005); J. Liu, J. Schmalian, and N. Trivedi, cond-mat/0411044 (unpublished).
[34] M. Tamura and R. Kato, J. Phys.: Condens. Matter **14**, L729 (2002).
[35] Y. Shimizu, K. Miyagawa, K. Kanoda, M. Maesato, and G. Saito, Phys. Rev. Lett. **91**, 107001 (2003).
[36] N. Elstner, R. R. P. Singh, and A. P. Young, Phys. Rev. Lett. **71**, 1629 (1993); N. Elstner, R. R. P. Singh, and A. P. Young, J. Appl. Phys. **75**, 5943 (1994).
[37] J. Oitmaa and E. Bornilla, Phys. Rev. B **53**, 14 228 (1996).
[38] R. Coldea, S. M. Hayden, G. Aeppli, T. G. Perring, C. D. Frost, T. E. Mason, S. W. Cheong, and Z. Fisk, Phys. Rev. Lett. **86**, 5377 (2001).
[39] P. Lacorre, J. Phys. C **20**, L775 (1987).
[40] O. Kahn, Chem. Phys. Lett. **265**, 109 (1997).
[41] D. Dai and M.-H. Whangbo, J. Chem. Phys. **121**, 672 (2004).
[42] For a review, see N. Elstner, Int. J. Mod. Phys. B **11**, 1753 (1997).
[43] A. B. Harris, C. Kallin, and A. J. Berlinsky, Phys. Rev. B **45**, 2899 (1992), see Fig. 14 and Eq. (4.5).

[44] A. J. Guttmann, in *Phase Transitions and Critical Phenomena*, edited by C. Domb and J. Lebowitz (Academic, New York, 1989), Vol. 13.
[45] D. L. Hunter and G. A. Baker, Jr., Phys. Rev. B **19**, 3808 (1979).
[46] M. E. Fisher and H. Au-Yang, J. Phys. A **12**, 1677 (1979).
[47] M. Shiroishi and M. Takahashi, Phys. Rev. Lett. **89**, 117201 (2002).
[48] S. Eggert, I. Affleck, and M. Takahashi, Phys. Rev. Lett. **73**, 332 (1994).
[49] J. K. Kim and M. Troyer, Phys. Rev. Lett. **80**, 2705 (1998).
[50] See, for example, N. Elstner, A. Sokol, R. R. P. Singh, M. Greven, and R. J. Birgeneau, Phys. Rev. Lett. **75**, 938 (1995).
[51] Y. Tokiwa *et al.* (unpublished).
[52] E. J. Rzepniewski, Ph.D. thesis, Oxford University, St. John's College, 2001.
[53] T. Nojiri (unpublished).
[54] R. Kato, N. Tajima, M. Tamura, and J-I. Yamaura, Phys. Rev. B **66**, 020508 (2002).
[55] T. Miyazaki and T. Ohno, Phys. Rev. B **59**, R5269 (1999).
[56] T. Komatsu, N. Matsukawa, T. Inoue, and G. Saito, J. Phys. Soc. Jpn. **65**, 1340 (1996).
[57] One should be cautious about taking Hückel and extended Hückel values as definitive. Based on comparison with results from the local-density approximation it has been argued [J. Merino and R. H. McKenzie, Phys. Rev. B **62**, 2416 (2000)] that the Hückel methods tend to systematically underestimate the hopping integrals.
[58] G. Visentini, M. Masino, C. Bellitto, and A. Girlando, Phys. Rev. B **58**, 9460 (1998).
[59] A. Fortunelli and A. Painelli, Phys. Rev. B **55**, 16 088 (1997).
[60] T. Nakamura, T. Takahashi, S. Aonuma, and R. Kato, J. Mater. Chem. **11**, 2159 (2001).
[61] A. H. MacDonald, S. M. Girvin, and D. Yoshioka, Phys. Rev. B **41**, 2565 (1990); **37**, 9753 (1988).
[62] G. Misguich, C. Lhuillier, B. Bernu, and C. Waldtmann, Phys. Rev. B **60**, 1064 (1999).
[63] R. Masutomi, Y. Karaki, and H. Ishimoto, Phys. Rev. Lett. **92**, 025301 (2004).
[64] W. LiMing, G. Misguich, P. Sindzingre, and C. Lhuillier, Phys. Rev. B **62**, 6372 (2000).
[65] R. Kato, Y. Kashimura, S. Aonuma, N. Hanasaki, and H. Tajima, Solid State Commun. **105**, 561 (1998); J. I. Yamaura, A. Nakao, and R. Kato, J. Phys. Soc. Jpn. **73**, 976 (2004)
[66] M. Capone, L. Capriotti, F. Becca, and S. Caprara, Phys. Rev. B **63**, 085104 (2000).
[67] P. Schiffer and I. Daruka, Phys. Rev. B **56**, 13 712 (1997).
[68] A. J. Garcia-Adeva and D. L. Huber, Phys. Rev. B **63**, 174433 (2001).
[69] R. Moessner and A. J. Berlinsky, Phys. Rev. Lett. **83**, 3293 (1999).
[70] J. Merino and R. H. McKenzie, Phys. Rev. B **61**, 7996 (2000).
[71] B. Bernu and G. Misguich, Phys. Rev. B **63**, 134409 (2001).
[72] O. I. Motrunich, cond-mat/0412556, Phys Rev. B (to be published 15 May 2005).
[73] S. S. Lee and P. A. Lee, cond-mat/0502139.